Modal analysis of the fields in the ITER ICRF antenna port plug cavity

Modal Analysis of the Fields in the ITER ICRF Antenna Port Plug Cavity

Fabrice Louche,[1, a)] Frédéric Durodié,[1] Alena Krivska,[1] Walid Helou,[2] and Daniele Milanesio[3]

[1)] *Laboratory for Plasma Physics-ERM/KMS, EURATOM-Belgian State Association, partner in the Trilateral Euregio Cluster, B-1000 Brussels, Belgium.*

[2)] *ITER Organisation, Route de Vinon-sur-Verdon - CS 90 046 - 13067 St Paul Lez Durance Cedex - France*

[3)] *Politecnico di Torino, Dipartimento di Elettronica, Torino, Italy*

[a)] *Corresponding author: fabrice.louche@rma.ac.be*

Abstract. The cavity that is formed between the ITER ICRF antenna plug and its port can exhibit resonances at specific frequencies, some of them in the relevant range of frequencies for IC heating. These resonances related to eigenmodes of the coaxial cavity, can substantially increase the level of electric fields inside the cavity and the level of RF losses in the B_4C neutron shielding tiles at the back of the port-plug cavity can also be significant. For instance, in MWS simulations of a simplified geometry of the antenna in front of a dielectric mimicking the plasma loading, the level of RF losses in the B_4C can reach tens of kW in $00\pi\pi$ toroidal phasing and even larger values in monopole. RF probes will be installed to monitor the RF fields in the port plug cavity and additional simulations are required to properly assess the integration (position, orientation) and their effectiveness. A model with a very detailed geometry of the antenna was also used in Ansys HFSS and TOPICA simulations. On the one hand it is observed that the resistivity of the B_4C neutron shielding material located at the back of the cavity has a marked effect on the excitation of the resonances and that for certain ranges of resistivity the numerical computation fails exhausting computer memory requirements (Ansys/HFSS) when trying to solve the total antenna and cavity problem as a single model. On the other hand lossy materials such as the B_4C tiles cannot be represented in TOPICA models while a realistic plasma gyrotropic load can not be simulated in HFSS/MWS. Therefore, we introduced a modal analysis in the cavity to decouple solving the computationally intensive plasma-facing front of the launcher from the cavity. The fields computed by TOPICA for various loading conditions and frequencies are evaluated on a set of vertical planes in the cavity and expanded in a series of modal eigenmodes for a given mode of operation. This provides the necessary input for an accurate evaluation of the RF fields in the cavity in an independent model not including the antenna front-face. It will also contribute to the understanding of the impact of the relative toroidal phasing of the strap currents on the excitation of the cavity modes and to simulate accurately the response of the cavity RF probes.

INTRODUCTION

The two ICRF antennas foreseen for ITER each consist of an array of 24 short radiating straps grouped in poloidal triplets (4 toroidally and 2 poloidally) through four-port junctions. The system will be operated between 40 and 55 MHZ and should deliver 20 MW per antenna. It might operate for various toroidal phasings for heating scenarios ($00\pi\pi$, $0\pi0\pi$ and $0\pi\pi0$). Current drive operations in $0\ \pi/2\ \pi\ 3\pi/2$ are also considered. The poloidal phasing is $-\pi/2$. The current status of the RF design of this antenna is reported in [1]. Each antenna is built as a whole assembly inside a port plug that is located within the vacuum vessel, and there is a gap around the antenna between the plug and the vessel. The presence of this gap can induce resonances of the coaxial type: the port plug acts as the inner conductor of a rectangular coaxial line, open on the front side and short-circuited at the back. In particular one of the possible cavity modes occurs in the range of frequency of interest for ICRF: a transverse electric (TE) mode is resonant around 45 MHz and leads to substantially large electric fields in the gap. This effect was observed in 3D numerical simulations [2, 3, 4] and was also validated experimentally with the help of a reduced-scale mock-up of the antenna [5, 6, 7]. As soon as the effect was identified, it was first considered to develop a grounding of the antenna plug in such a way to reduce the electrical length of the cavity and move the resonance out of the ICRF range. But mechanical considerations made these grounding solutions unpractical and unacceptable, and it was rather decided to monitor the RF fields in the cavity with the help of RF probes in order to be able to avoid deleterious effects, if any. In a recent series of simulations [8] a more realistic geometry of the cavity that includes the doglegs and the B_4C neutron shielding tiles located at the back of the port-plug cavity was considered, and the impact of the various toroidal phasings on the level of excitation of the cavity modes was studied. In particular it was shown that the level of RF losses in the B_4C can reach tens of kW in $00\pi\pi$ toroidal phasing and even larger values in monopole. These simulations were performed with the 3D electromagnetic commercial software CST Microwave Studio (MWS), with the approximation of a dielectric loading to emulate a plasma. If the inclusion of a magnetized plasma into CST is

possible, it requires computer ressources not available to the authors at the time of writing. On the contrary, the plasma coupling code TOPICA [9, 10] not only allows for realistic plasma profiles, but also the code has been parallelized and optimized and therefore it can simulate a very detailed model of the ITER antenna including a PEC (Perfectly Electric Conducting) cavity. A limitation of the code is the impossibility to properly represent lossy materials, a requirement to compute accurate values of the RF losses in the B_4C tiles. Another tool frequently used for antenna simulations is the Ansys/HFSS commercial package. It can represent lossy materials, but it was observed that for certain ranges of resistivity the numerical computation fails exhausting computer memory requirements when trying to solve the total antenna and cavity problem as a single model.

Therefore, we introduce in the present work a modal analysis in the cavity to decouple solving the computationally intensive plasma-facing front of the launcher from the cavity: see Fig. 1.

Remark: the B_4C layer is here assumed to directly attach to the surface of the cavity. At the time of writing it is not yet clear if this layer will be exposed or if the option of coating it with some high conductivity material will be explored.

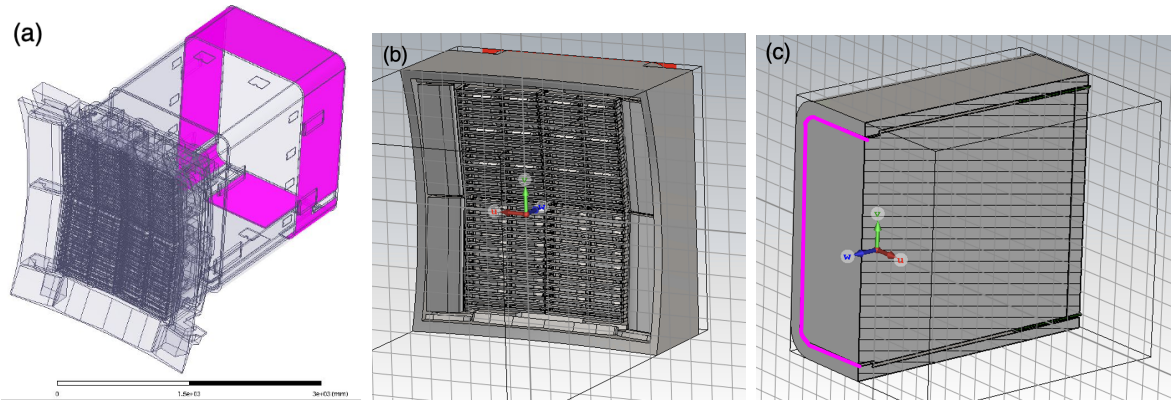

FIGURE 1. Full and decoupled models of the ITER ICRF antenna used in the TOPICA/HFSS/MWS simulations; (a): full geometry including the port plug cavity highlighting surfaces of the B4C neutron shielding; (b): front face; (c): transverse cut view of the cavity (short-circuited at the right side). The cavity port on which the modes will be evaluated is highlighted in pink.

MODAL ANALYSIS: METHODOLOGY AND ASSUMPTIONS

A general theory for the full spectrum of modes in a cavity can be found in [11, 12]. Any function defined in a closed region Ω (a "cavity") can be expanded in a series of orthonormal functions of two types: the irrotational modes and the solenoidal modes. Equivalently, the Helmholtz equation

$$\nabla \times (\nabla \times \mathbf{E}) - \omega^2 \varepsilon \mu^{-1} \mathbf{E} = 0 \text{ in } \Omega \tag{1}$$

with the boundary equation $\vec{n} \times \mathbf{E} = 0$ on $\partial\Omega$ admits two types of solutions. The irrotational field solutions are characterized by the conditions $\nabla \times \mathbf{E_{ir}} = 0$ in Ω and $\vec{n} \times \mathbf{E_{ir}} = 0$ on $\partial\Omega$ Consequently irrotational modes are generated from a scalar function. The solenoidal solutions have the properties $\nabla \bullet \mathbf{E_s} = 0$ and $\vec{n} \times \mathbf{E_s} = 0$ on $\partial\Omega$. Irrotational modes and solenoidal modes have the property to be mutually orthogonal. Therefore these sets of solution represent a basis in the Hilbert space of wave fields in Ω, and any electric field in the cavity can be expanded in terms of $\mathbf{E_s}$ and $\mathbf{E_{ir}}$.

For the presently considered case of a rectangular coaxial cavity with perfectly conducting walls, the solenoidal modes reduce to the usual TE and TM (transverse magnetic) modes while the only irrotational mode is the transverse electro-magnetic mode (TEM). Therefore, any electric field $\mathbf{E_{RF}}$ in the cavity can be expanded in the basis $\{\widehat{\mathbf{e_n}}\}$ of the cavity modes:

$$\mathbf{E_{RF}} = A\mathbf{E_{TEM}} + \sum_n B_n \mathbf{E_{TE,n}} + \sum_m C_m \mathbf{E_{TM,m}} = \sum_n A_n \widehat{\mathbf{e_n}} \tag{2}$$

Any RF field $\mathbf{E_{RF}}(x,y)$ will excite a given mode n according to a certain weight defined by the following surface integral

$$A_n = \iint_S \mathbf{E_{RF}} \widehat{\mathbf{e_n}}^* dS \tag{3}$$

where S is the gap cross-section. In Fig.1 the ITER ICRF antenna geometry has been cut in two parts: the plasma-facing front (including a few blanket shield modules) on the one hand, and the back cavity on the other hand. Any RF field tangential to the interface between the two half-models can be expanded in a series (2) of cavity eigenmodes.

Considering the aspect ratio gap width to gap circumference it is assumed that the E fields of the TEM and TE modes are relatively constant across the gap width so that the 2-dimensional integral of E-field distributions (3) can be replaced by a line integral of the value of these fields on a line running in the middle of the port gap between the plug and the port perpendicular to the cavity axis, see Fig. 2(a). This approach is more practical than rigorously computing surface integrals over the port gap of products of E-fields to extract the mode content (see below) all the more so because the resolution with which the E-fields can be extracted from the TOPICA runs is rather limited. It is further assumed that the field variation across the gap is negligible and that the fields (be it the total or modal field distributions) are aligned with the unit vector $\widehat{\mathbf{1}_\xi}$ normal to the central curve so that the integral of field across the gap is approximated by:

$$A_n \simeq \iint_S \mathbf{E_{RF}} \widehat{\mathbf{e_n}}^* ds d\xi \simeq \iint_S \left[E_{RF,\xi} \widehat{\mathbf{1}_\xi}\right] \left[e^*_{n,\xi} \widehat{\mathbf{1}_\xi}\right] ds d\xi \simeq \oint g(s) E_{RF,\xi}(s) e^*_{n,\xi}(s) ds \tag{4}$$

where $g(s)$ is the length of the gap, $E_{RF,\xi}(s)$ and $e_{n,\xi}(s)$ are the normal components of the RF and the mode electric fields respectively. In order for the decomposition to work properly the base of $\{\widehat{\mathbf{e_n}}\}$ must be orthonormal: $\oint g(s) e_{m,\xi} e^*_{n,\xi} ds = \delta_{mn}$. As the eigenmodes are typically computed for a given incident power, they need first to be normalized.

Once the modal content, i.e. the vector $\mathbf{A}$ of components A_n, is known in a given cross-section, the spectrum of forward waves exciting the cavity and backward waves reflected from the cavity can be determined: $\mathbf{E} = \sum_n \alpha_n \widehat{\mathbf{e_n}}(x,y) e^{\gamma z} + \beta_n \widehat{\mathbf{e_n}}(x,y) e^{-\gamma z}$, where γ is the wave propagation constant. The multimodal scattering matrix of the cavity $\mathbf{S}$ connects the incident and reflected waves: $\beta_n = \sum_k \mathbf{S}_{nk} \alpha_k$. At $z = 0$, we can easily show that $\alpha = (\mathbf{S} + \mathbf{I})^{-1} \mathbf{A}$, where $\mathbf{I}$ is the identity matrix. In practice the $\mathbf{S}$ matrix can be computed once for all (with MWS or HFSS) for a given cavity geometry by defining a waveguide port at its front (highlighted in pink in Fig. 1(C)). The same model can later be simulated with a proper excitation $\{\alpha_n\}$ to assess the level of RF fields and losses, for given frequency, plasma profile, and toroidal phasing. The inverse strategy is also possible: the front can be calculated once for a given loading and then the effects of variations of the cavity properties (e.g. resistivity of B_4C) can be computed.

MODELING RESULTS: MODAL CONTENT

The antenna geometry is displayed in Fig. 1, and corresponds to the so-called "CY12FS2str2" geometry, it being the current reference model. This geometry was run with TOPICA for various reference plasma density profiles [10]. The cavity eigenmodes were determined with HFSS on a homogeneous extension by 250mm of the port-plug cavity port face (the pink face in Fig. 1(c)) where the opposite face was terminated on a matched waveguide port in such a way to eliminate reflections. The profiles of the electric fields of the TEM mode and the first three TE modes along the curved line centred in the gap between the plug and the port have been plotted in Fig. 2(b).

We show in Fig. 3(a) one example of a field map obtained from the TOPICA results, for the "LowCut" plasma profile at 55 MHz for $00\pi\pi$ toroidal phasing and the usual $0 - \pi/2$ poloidal phasing. The plane where the modal content of the fields is evaluated is indicated on the figure. The magnitude of the electric field along the reference curve in the gap is plotted in Fig. 3(b) for the same phasing and in $0\pi\pi0$. It should be noted that the discontinuities visible on these curves are due to some inaccuracies in the TOPICA results around the corners of the plug. Nevertheless they have a negligible impact on the results of the present analysis.

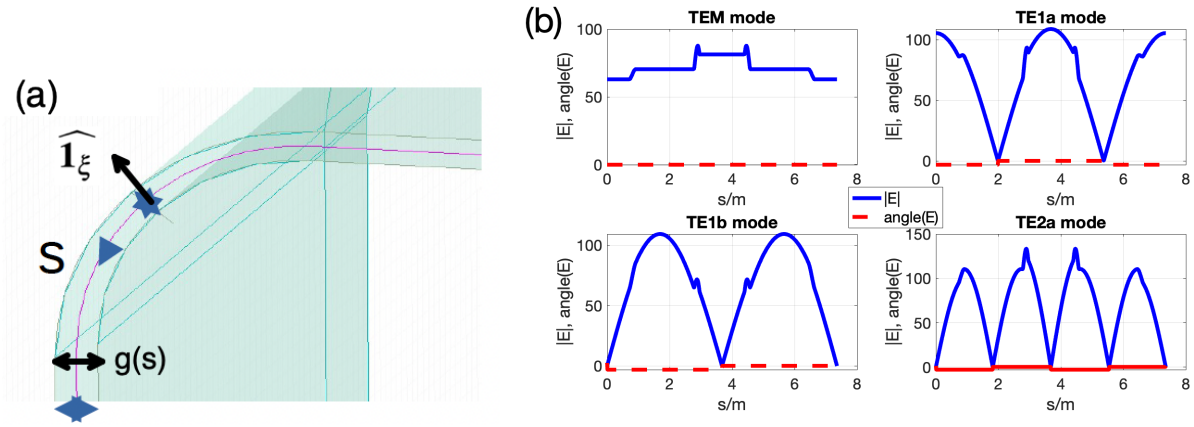

FIGURE 2. (a): detail of the curved line centred between the plug and the port along which the electric fields of the cavity modes are evaluated; local gap $g(s)$ and normal vector $\widehat{1_\xi}$ are also visible; (b)-: electric field profiles (magnitude and phase) along the curve for the first four cavity modes. The zero of the s axis is the center of the bottom horizontal section of the gap, and it goes clockwise along the curve.

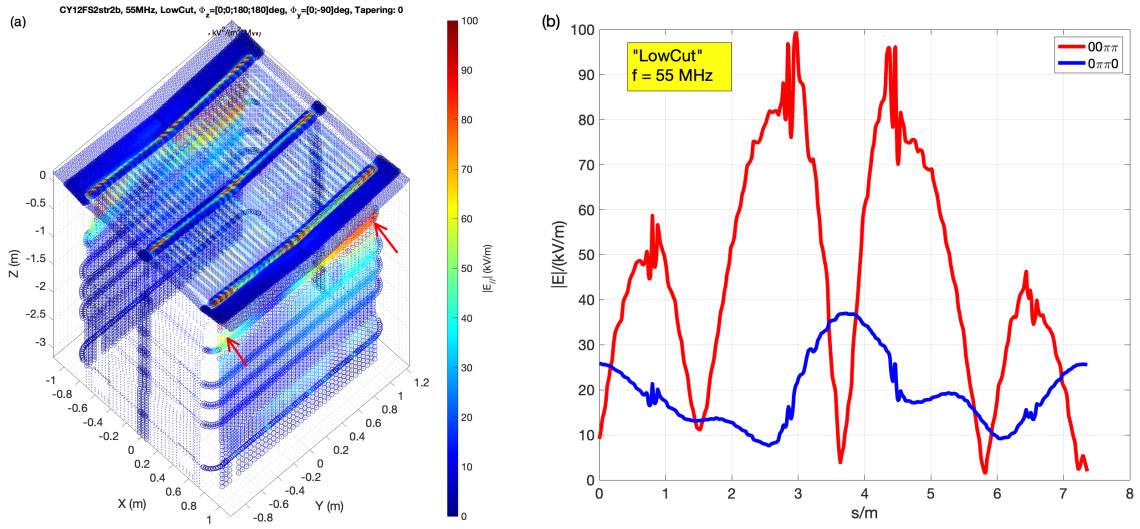

FIGURE 3. Tangential electric fields computed by TOPICA for "LowCut" plasma profile at 55 MHz; (a) 3D map of the fields in $00\pi\pi$ in front of the array and in the cavity (the two red arrows indicate the plane where the TOPICA fields are evaluated for determining their modal content; (b) tangential electric field in the reference plane and along the curve depicted in Fig. 2(a) in $00\pi\pi$ and $0\pi\pi0$

Let us first discuss the modal expansion of the fields in $0\pi\pi0$ phasing for various frequencies: Fig. 4 shows the components A_n for the first 9 eigenmodes, for various plasma profiles. It should be noted that 47.5 MHz is the frequency value which is the closest to the resonance frequency. From these figures we can clearly see that the mode TE_{1a} is mostly excited in most of the considered profiles and at most frequencies. In particular, at the resonance, this mode is the dominant term, with an amplitude one order of magnitude larger than at the other frequencies. It makes perfect sense as this mode has its maxima and minima at the level of the vertical and horizontal mid-planes, similarly to the TOPICA field. We also observe a direct amplification of the mode excitation at resonance as the coupling conditions are decreasing, as the case "LowCut+150cm" is practically equivalent to a vacuum loading case. This effect was also observed in [8]: the level of RF losses in the B_4C layer, used as a measure of the excitation of RF fields in the cavity, would clearly be larger in vacuum than with a dielectric medium in front of the antenna, but only in monopole and $0\pi\pi0$. Another intriguing result at the non-resonant frequencies is that for the profiles with the

largest coupling, i.e. "High+4cm" and "Case4IPP", the TEM and TE_{1b} modes contribute strongly to the expansion, and even dominate above the resonance. This perturbation of the RF electric field from a typical TE_{1a} shape to a TE_{1b} which is the type of profile expected from a dipole toroidal phasing is correlated with the amount of power coupled to the plasma: see Fig. 5. It could be that the reduced SOL-antenna distance of good coupling profiles enhances strap mutual coupling and perturbates the distribution of the fields. A more detailed analysis of the near-fields in front of the ICRF antenna for varying profiles is required to fully understand this result. Also this perturbation of the near-fields is not visible at 47.5 MHz, so the resonant amplification of mode TE_{1a} dominates the other contributions in the modal expansion.

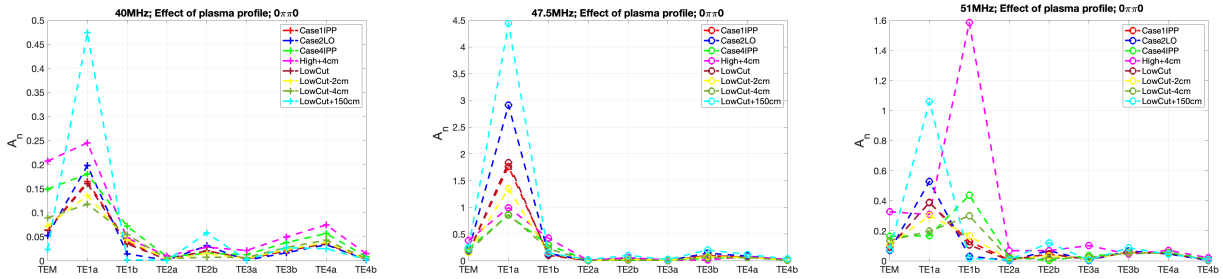

FIGURE 4. Modal content of the RF electric field in the reference plane for a set of plasma profiles in $0\pi\pi0$ toroidal phasing: coefficient A_n defined by (4) for the first eigenmodes of the cavity. From left to right: 40 MHz, 47.5 MHz (close to resonance) & 51 MHz.

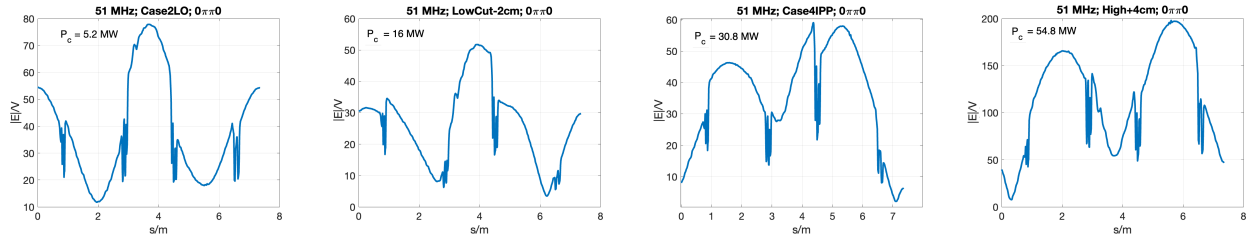

FIGURE 5. Profile of the RF electric field in V along the reference loop curve in the gap at 51 MHz in $0\pi\pi0$ for 4 plasma profiles in increasing order of coupled power P_C (indicated on each plot).

We now perform the same analysis for $00\pi\pi$ toroidal phasing, see Fig. 6 for the respective modal expansions. At the resonance the TE_{1b} is mostly excited, as expected, but we notice that for the two high coupling profiles "Case4IPP" and "High+4cm", the mode TE_{1b} is substantially more amplified and dominates the spectrum for these profiles. We have plotted in Fig. 7 the variation of the electric field amplitude along the curve in the gap, and we clearly observe the same pattern, i.e. a correlation between the coupled power and perturbation of the field in the gap, which behaves more like a TE_{1a} mode as the coupled power is increasing. Interestingly the situation at 51 MHz is closer to what we would expect for a resonance for these very high coupling cases. The toroidal phasing has an impact on the resonance frequency, as was observed in all previous works on the subject (see for instance [2, 7, 8]). But the loading conditions are not expected to modify the value of this frequency (in particular by a couple of MHzs as observed here), the resonance being a reactive effect.

CONCLUSION

A method has been developed to extract from TOPICA outputs the electric fields in the gap of the ITER ICRF antenna port plug and to compute their expansion in eigenmodes, for various frequencies and plasma profiles. Depending on the toroidal phasing, one mode dominates the expansion and is preferentially excited in the cavity: the TE_{1a} mode in monopole and $0\pi\pi0$ phasing, and the TE_{1b} mode in dipole phasings ($00\pi\pi$ and $0\pi0\pi$). Nevertheless a systematic dependance in the plasma profile was observed, as high coupling profiles tends to perturb the expansion and to excite

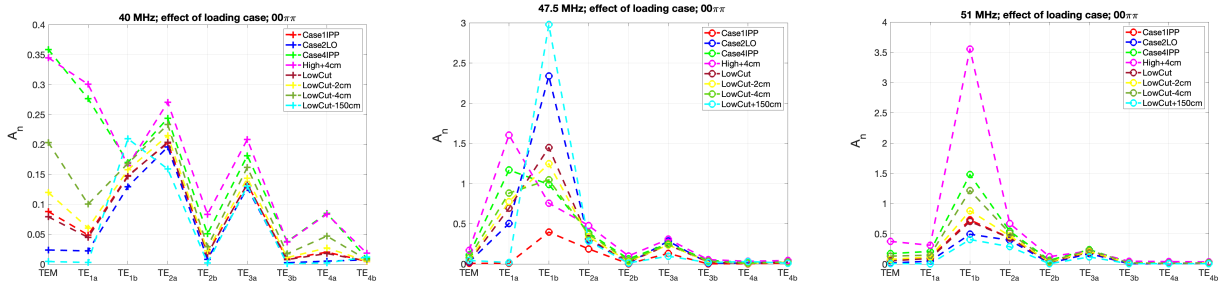

FIGURE 6. Modal content of the RF electric field in the reference plane for a set of plasma profiles in $00\pi\pi$ toroidal phasing: coefficient A_n defined by (4) for the first eigenmodes of the cavity. From left to right: 40 MHz, 47.5 MHz (close to resonance) & 51 MHz.

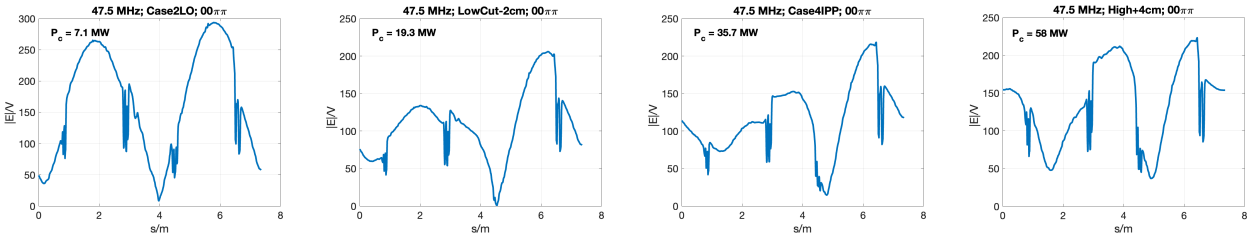

FIGURE 7. Profile of the RF electric field in V along the reference loop curve in the gap at 47.5 MHz in $00\pi\pi$ for 4 plasma profiles in increasing order of coupled power P_C (indicated on each plot).

higher order eigenmodes. If it is very likely that this effect is due to non trivial effects induced by enhanced mutual coupling, further analysis of the TOPICA outputs is required to correctly understand the results. In the meantime the spectrum of forward excitations at the port of the cavity decoupled from the front face has been evaluated and results should be ready in a near future.

ACKNOWLEDGMENTS

This work has been conducted under contracts IO/20/CT/4300002118 and IO/20/CT/4300002178.
The views and opinions expressed herein do not necessarily reflect those of the ITER Organization.

REFERENCES

1. B. Beaumont, "Status of the ITER ion cyclotron H&CD," EPJ Web of Conferences 157, 02002 (2017) **157**, 02002 (2017).
2. F. Louche et al., "Eigenmode analysis of the ITER ICRF antenna plug and electrical solution to the grounding of the antenna," Nucl. Fusion **49**, 065025 (11pp) (2009).
3. F. Louche et al., "Influence of the blanket shield modules geometry on the operation of the ITER ICRF antenna," Fusion Engineering and Design **88**, 926–929 (2013).
4. F. Durodié et al., "Design, performance, and grounding aspects of the ITER ICRF antenna," Phys. Plasmas **21**, 061512 (2014).
5. P. Dumortier at al., "Validation of the electrical properties of the ITER ICRF antenna using reduced-scale mock-ups," Radio Frequency Power in Plasmas - AIP Conf. Proc. **1406**, 29–36 (2011).
6. P. Dumortier at al., "ITER ICRH antenna grounding options," Fusion Engineering and Design **88**, 922–925 (2013).
7. P. Dumortier at al., "Further studies on the ITER ICRF antenna grounding," AIP Proceedings **2254**, 070013 (2020).
8. F. Louche, "Simulation for the cavity modes," Report on Task 1.a for the IO contract IO/20/CT4300002178 (2021).
9. V. Lancelotti et al., "TOPICA: an accurate and efficient numerical tool for analysis and design of ICRH antennas," Nucl. Fusion **46**, S476–S499 (2006).
10. D. Milanesio et al., "Recent analysis of the ITER ion cyclotron antenna with TOPICA code," these proceedings (2022).
11. K. Kurokawa, "The expansions of electromagnetic fields in cavities," IRE Trans. Microwave Theory Tech. **6**, 178–187 (1958).
12. R. E. Collin, *Field Theory of Guided Waves*, edited by J. Wiley-Interscience (IEEE Press, 1991).